Stability Analysis of Flying-capacitor Linear Amplifier for Wireless Power Transfer system

Rintaro Kusui[1*], Keisuke Kusaka[2] and Jun-ichi Itoh[1]

1 Department of Science of Technology Innovation, Nagaoka University of Technology, Nagaoka, Japan
2 Dept. of Electrical, Electronics and Information Engineering, Nagaoka University of Technology, Nagaoka, Japan
*E-mail: kusui@stn.nagaokaut.co.jp

Abstract— **In this paper, the stability of a flying-capacitor linear amplifier (FCLA) for wireless power transfer systems is analyzed by a small-signal equivalent circuit. A wideband width controller for FCLA is needed to output the high-frequency voltage for a wireless power transfer system. The output voltage of the FCLA is controlled by the analog gate voltage with operational amplifiers on a controller. Due to this, it is necessary to analyze the stability of FCLA, including the frequency characteristics of the operational amplifiers. The maximum stable gain is analyzed with the small-signal equivalent circuit. Then, the harmonics of the output current of a 4-series FCLA with an unfolder are analyzed by a simulation. As a result, the harmonic components are reduced by 40 dB or more than the fundamental component.**

Keywords— *Flying-capacitor linear amplifier, wireless power transfer, stability analysis, small-signal equivalent circuit*

I. INTRODUCTION

In recent years, electric vehicles (EVs) have become increasingly popular to reduce emissions of greenhouse gases such as NOx gas, one of the causes of global warming. The batteries in electric vehicles have a lower energy density than those in conventional gasoline-powered vehicles, so they require frequent recharging. Therefore, wireless power transfer (WPT) systems that enable easy and safe recharging are being actively studied [1–3]. The WPT systems improve user convenience because charging is initiated without cumbersome power cable connections. However, the WPT with electromagnetic induction transmits power through very weak magnetic coupling, which causes a large leakage magnetic field around the transmission coil. Leaky magnetic fields may cause malfunctions of surrounding electronic equipment and wireless communication failures. Therefore, it is necessary to satisfy the regulations set by each country based on the guidelines [3–4] set by the International Special Committee on Radio Interference (CISPR). In particular, a revision of the guideline for WPT systems is under consideration by CISPR11. Specifically, a reduction of about 30 dB in the 150 kHz to 30 MHz range, which corresponds to the low-order harmonic component of WPT systems, is being considered [5]. For this reason, it is necessary to develop a method to reduce leakage magnetic fields, especially low-order harmonic components, in WPT systems.

Conventional WPT systems use an inverter that outputs a square wave voltage as the primary power source [6].

Because the square wave voltage output by the inverter contains low-order harmonic components, a current also contains low-order harmonic components that flow on the coils even if resonant circuits are used. This harmonic current causes leakage magnetic fields containing harmonic components to be radiated from the transmission coil.

Magnetic shielding methods using metals, magnetic materials, and additional windings have been proposed in order to reduce leakage magnetic fields [7–9]. In these methods, a current flows when the leakage magnetic field is interlinked to the shielding material, thereby reducing the leakage magnetic field. Thus, the current in the shielding must be larger to obtain a larger shielding effect, which causes an increase in losses on the WPT system.

The authors have proposed a flying capacitor linear amplifier (FCLA) as the primary power supply of a WPT system [10–13] to reduce the radiation noise harmonics. The FCLA allows a significant reduction in leakage field harmonics generated by the WPT system. The gate drive circuits for FCLA are connected to each MOSFET to keep balancing the flying capacitor (FC) voltages while controlling the output voltage using a proportional controller. However, a wideband controller is needed to control the high-frequency voltage used in WPT systems.

In this paper, the bandwidth of the FCLA is analyzed from the small-signal equivalent circuit of the MOSFET, and the stability of the FCLA, including the bandwidth of the controller, is analyzed. From the analysis results, we demonstrate by simulation that the FCLA with the designed control gain can output high-frequency voltage stably.

II. FLYING CAPACITOR LINEAR AMPLIFIER

A. Circuit Configuration

Figure 1 shows the configuration of a WPT system. The FCLA is used in the primary power supply. The power supply circuit consists of an *n*-series FCLA with *n* N-channel MOSFETs (n-MOSFETs), *n* diodes connected in series, and the unfolder. An *n*-series FCLA outputs a full-wave rectification voltage, and by switching polarity with the polarity switching circuit, a voltage without harmonics is applied to the transmission coil. The FCLA output only a positive current by switching the polarity in the unfolder. The p-MOSFET, which has inferior characteristics

compared to the n-MOSFET, operates in an active state when negative current flows. For this reason, the p-MOSFET is replaced by a diode, with the addition of an unfolder. This improves efficiency and output waveform distortion.

Figure 2 shows the operating region of an n-MOSFET, which is divided into on, off, and active states according to the drain-source and gate-source voltages. Conventional inverters use only the on-state with low drain-source voltage and the off-state with no current flow. On the other hand, the FCLA output any continuous voltage using one of the MOSFETs connected in series in the active state. Conventional push-pull linear amplifiers have a low maximum efficiency of 78.5%, making it difficult to increase transmission power. On the other hand, the FCLA is driven at high efficiency by connecting MOSFETs in series, which reduces the applied voltage to the MOSFETs and the losses caused by the active operation. An analog voltage must be input between gate source to use the MOSFETs in active state for FCLA to output any continus voltage..

B. Controllor Configuration

Figure 3 shows a block diagram for controlling output voltage and operating state. The output voltage is controlled by a proportional controller. The proportional controller outputs a gate-source voltage command value. Each gate driver inputs the gate source voltage command output by the controller to MOSFET and adds an offset to select the operation region. FCLA has the cominations of operational state which output same voltage and have different current path. Due to this, the flying-capacitor (FC) voltages are balanced by selecting the appropriate combination of operating state, i.e., current path.

C. Voltage Balancing for Flying Capacitor

Figure 4 shows the state selection of MOSFETs using phase-shifted carriers in a 4-serial FCLA; the FCLA keeps balancing of the FC by appropriately selecting the operating state of each MOSFET. In this system, the state of each MOSFET is selected by phase-shifted carrier comparison, which is also used in conventional flying capacitor converters. The frequency of the carrier is asynchronous to the output frequency so that the combination of the selected operating states changes in one output cycle to balance the FC voltage for a long period. If the FC voltage becomes unbalanced due to disturbances, etc., the voltage controller transitions the operating states to maintain the voltage balance [13].

III. STABILITY ANALYSIS OF FCLA

A. Open-loop Characteristic of FCLA

Figure 5 shows the small-signal equivalent circuit of the FCLA. The FCLA is linearized using the transfer conductance g_m and the output resistance r_o representing the channel length modulation to analyze the frequency response. In addition, parasitic capacitances among drain,
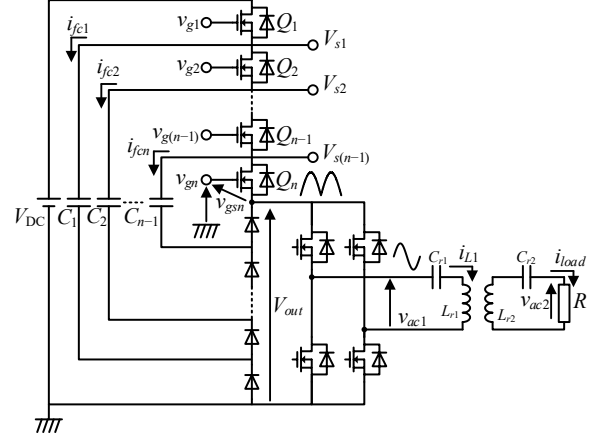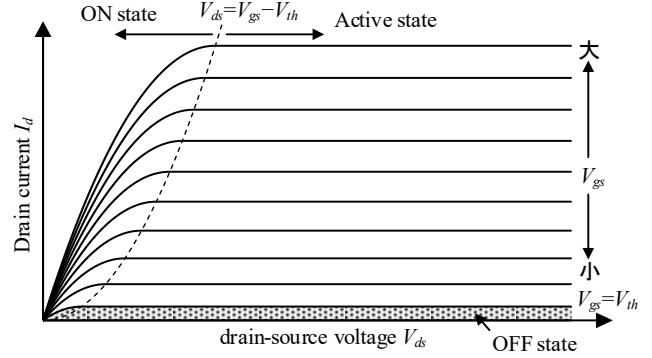

Fig. 1. FCLA for WPT system.

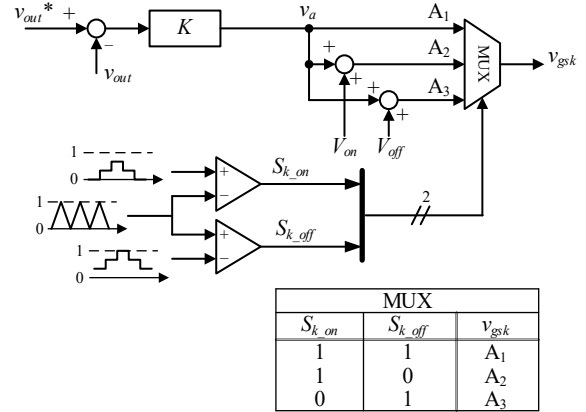Fig. 2. Operation region of n-MOSFET.

MUX		
S_{k_on}	S_{k_off}	v_{gsk}
1	1	A_1
1	0	A_2
0	1	A_3

Fig. 3. Block diagram of output voltage controller.

source and gate are added to the small-signal equivalent circuit of the MOSFTE to represent the frequency response. Since the FCLA is based on a source follower circuit with the class-B operation, the equivalent circuit has the same form as the source follower circuit. In the case of a source follower circuit, DC voltage is ignored in small-signal circuits. On the other hand, in the case of the FCLA, the DC voltage is represented as a disturbance component because the DC voltage appears to vary with the range of output voltage. Based on these assumptions, the transfer function G_{FCLA} from the input voltage v_{in} between the gate and source terminals to the output voltage v_{out} is given by

$$G_{FCLA} = \frac{K\omega_n^2(1 - sT_h)}{s^2 + 2\zeta\omega_n s + \omega_n^2} \tag{1}.$$

where each coefficient K, T_h, ω_n, ζ are expressed by (2–5).

$$K = \frac{g_m r_o R}{r_o + R} \tag{2}$$

$$T_h = \frac{c_{gd}}{r_o} \tag{3}$$

$$\omega_n = \frac{1}{\sqrt{r_g \dfrac{r_o R}{r_o + R}(C_{gs}C_{ds} + C_{ds}C_{gd} + C_{gd}C_{gs})}} \tag{4}$$

$$\zeta = \frac{\dfrac{r_o R}{r_o + R}\left\{(1 + r_g g_m)C_{gd} + C_{ds}\right\} + r_g(C_{gd} + C_{gs})}{\sqrt{r_g \dfrac{r_o R}{r_o + R}(C_{gs}C_{ds} + C_{ds}C_{gd} + C_{gd}C_{gs})}} \tag{5}$$

B. Closed-loop Characteristic of FCLA without limited bandwidth for operational amplifiers

Figure 6 shows a block diagram of the FCLA voltage control system with the operational amplifiers which has limited bandwidth. The FCLA requires an analog voltage to be applied between the gate and source of each MOSFET according to the output voltage or current to use the MOSFETs in an active state. Thus, the control circuit and gate drive circuit are implemented as analog circuits using operational amplifiers. For this reason, it is necessary to analyze the system including the operational amplifier bandwidth in order to analyze the stability of the FCLA voltage control. In Fig. 6, G_{amp} indicates the transfer function of the op-amps, the number of op-amps in the amplification and drive sections and the number of op-amps in the detection part. First, the control response is evaluated when the ideal op-amp ($G_{amp} = 1$) is used. If the proportional gain of feedback is K_p, the transfer function G_c from the command value v_{out}* to the output voltage v_{out} is given by

$$G_c = \frac{K_p G_{FCLA}}{1 + K_p G_{FCLA}} = \frac{K_c \omega_{nc}^2(1 - sT_h)}{s^2 + 2\zeta_c \omega_{nc} s + \omega_{nc}^2}$$
(6).

where each coefficient is expressed by equations (7–9).

$$K_c = \frac{K_p K}{1 + K_p K} \tag{7}$$

$$\omega_{nc} = \omega_n \sqrt{1 + K_p K} \tag{8}$$

$$\zeta_c = \frac{2\zeta - K_p K \omega_n T_h}{2\sqrt{1 + K_p K}} \tag{9}$$

Equation (6) shows that the closed-loop characteristics of the FCLA with proportional control is expressed as the sum of a first-order phase lead element and a second-order phase delay element. The damping ratio ζ_c shown in (9) must be positive for stable control of FCLA. Thus, the proportional gain K_{p_lim} of the stability limit is expressed
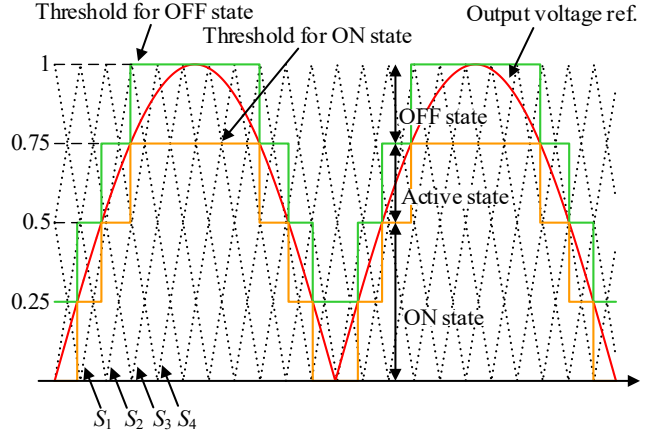

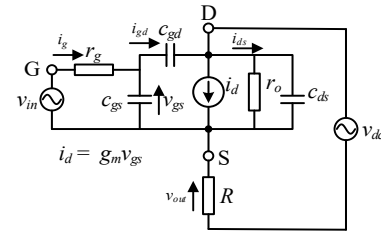Fig. 4. State selection by comparing with phase-shifted carrier for 4-series FCLA.

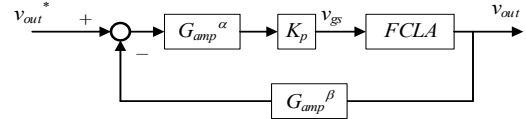Fig.5. Small signal equivalent circuit model of FCLA.

Fig. 6. Control block diagram with op-amp for detection and amplify.
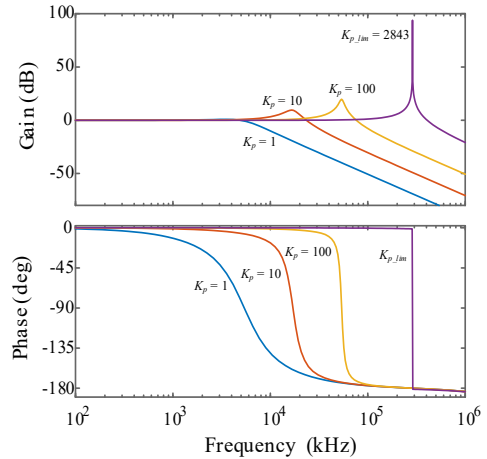

Fig. 7. Close-loop characteristic with ideal op-amps.

as (10), and the control bandwidth ω_{nc_max} at that time is obtained as equation (11).

$$K_{p\_lim} = \frac{2\zeta}{K\omega_n T_h} \tag{10}$$

$$\omega_{nc\_max} = \omega_n \sqrt{1 + \frac{2\zeta}{\omega_n T_h}} \tag{11}$$

Figure 7 shows the closed-loop characteristics when the proportional gain is varied. From Fig. 7 and equations (8) and (9), it can be seen that the natural angular f requency

ω_c increases as the gain is increased. On the other hand, increasing the gain makes the braking coefficient ζ_c smaller, resulting in an oscillatory response.

C. Closed-loop Characteristic of FCLA with limited bandwidth for op-amps

In this section, the stability of the FCLA including operational amplifiers with limited bandwidth is analyzed. The operational amplifier is expressed as a second-order low-pass filter, so the transfer function becomes (12). In this system, a current feedback operational amplifier is used, and the bandwidth can be set regardless of the gain of the amplifier circuit by appropriate selection of the feedback resistor. From the above, all operational amplifiers constituting the controller are expressed by the transfer function in equation (12), and the gain is all collectively denoted as K_p.

$$G_{amp} = \frac{\omega_{amp}^2}{s^2 + 2\zeta_{amp}\omega_{amp}s + \omega_{amp}^2} \qquad (12).$$

where ω_{amp} is the natural angular frequency of the operational amplifier and ζ_{amp} is the damping factor of the operational amplifier.

Figure 8 shows the control circuit and gate drive circuit used in this system. The control circuit consists of a detection section, a command value input section, an amplification section, a state selection section, and a drive section. Of these, the detection, amplification, and drive sections affect the control characteristics. Two operational amplifiers are connected to the detection stage, two to the amplification stage, and one to the drive unit. Therefore, the transfer function that takes into account the bandwidth of the operational amplifiers is expressed by Equation (13).

$$G_{camp} = \frac{G_{FCLA}G_{amp}^3}{1 + G_{FCLA}G_{amp}^5}$$

$$= \frac{K_p K \omega_n^2 \omega_{amp}^6 (1 - sT_h)(s^2 + 2\zeta_{amp}\omega_{amp}s + \omega_{amp}^2)^2}{(s^2 + 2\zeta_n s + \omega_n^2)(s^2 + 2\zeta_{amp}\omega_{amp}s + \omega_{amp}^2)^5 + K_p K \omega_n^2 (1 - sT_h)\omega_{amp}^{10}}$$

$$(13).$$

Figure 9 shows the open-loop and closed-loop characteristics of the system shown in equation (13) when the gain is varied in (a) and (b), respectively. Figure 9(a) shows that the phase changes significantly due to the influence of the operational amplifier and that the phase margin decreases even at low gain. Figure 9(b) shows that the bandwidth is similar with and without the op-amp for low gains where the margins are high, and the bandwidth is sufficiently far from the op-amp bandwidth. It can also be confirmed that even the stable gain without the op-amp is unstable due to the decrease in the stability margin.

From the above results, it is confirmed that the bandwidth of the FCLA can be designed by separating the bandwidth of the FCLA from that of the op-amp sufficiently, rather than the transfer characteristics without considering the op-amp.
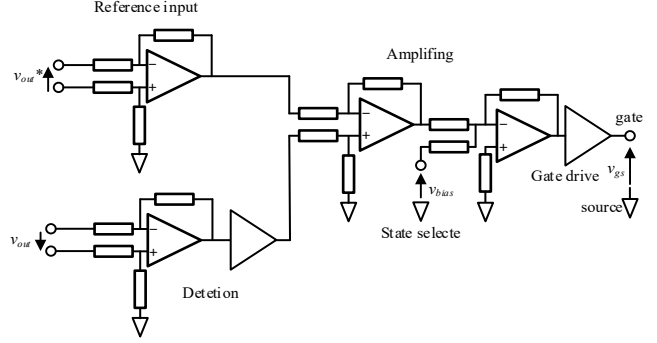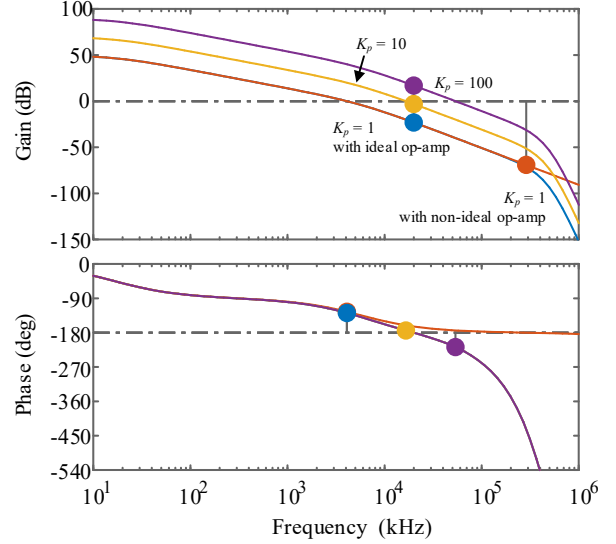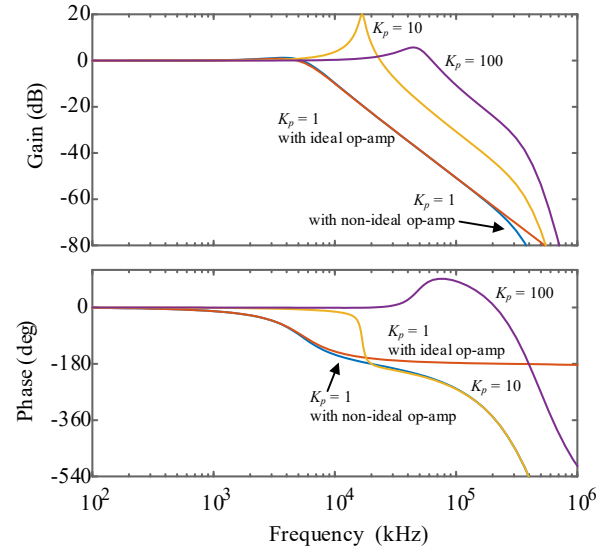

Fig. 8. Circuit diagram of voltage controller and gate driver.

(a) Open-loop characteristic

(b) Close-loop characteristic

Fig. 9. Bode diagram of small signal equivalent circuit for FLCA.

IV. SIMULATION RESULT

Figure 10 shows the operating waveforms of the source follower circuit. Figure 10 shows the source voltage and gate-source voltage simulated by a linearized small-signal equivalent circuit of a MOSFET and a SPICE model of a MOSFET, respectively. The command value is a sine

wave of 85 kHz with an offset of half of the DC voltage, for Class-A operation. From Figure 10, it can be seen that the output voltage is equal for both models. The gate-source voltage input to output the same voltage is also approximately the same, indicating that the linearized small-signal equivalent circuit is valid. This is because the small-signal equivalent circuit ignores the small-signal equivalent circuit.

Figure 11 shows the circuit configuration of the FCLA to be simulated. The simulation circuit is a 4-serial FCLA with a polarity switching circuit and a resistor connected as a load. 160 V DC voltage is set so that the applied voltage per MOSFET is about 40 V since the withstand voltage of the MOSFET is 60 V. The output voltage command was a full-wave rectified voltage with an amplitude of 160 V and an output frequency of 85 kHz.

Figure 12 shows the operating waveforms. The simulation is simulated using a second-order LPF so that the number of operational amplifiers is the same as that used in the system. Figure 12 shows that the system operates stably with the gain analyzed by the small-signal circuit model. However, near the zero-crossing of the full-wave rectification voltage, the output voltage cannot be adequately controlled and is distorted. This is because a very high control bandwidth is required at the point where the output voltage becomes discontinuous.

Figure 13 shows the output current harmonics analysis results of the polarity switching circuit. When applied to a WPT system, it is the current that causes the leakage magnetic field. Therefore, the output current harmonics of the unfolder are analyzed. In the simulation, a voltage with an amplitude of 160 V is applied to the resistance of the load24. Therefore, the RMS value of the fundamental current is 4.71 A (13.5 dBA). From Figure 13, it can be confirmed that the fundamental component of the current is 4.71 A. The harmonic component can be reduced by more than 40 dB.

V. EXPERIMENTAL RESULT

Figure 14 shows the configuration of the test circuit. The test circuit is a source follower equivalent to a single-series FCLA. The DC voltage is set to 30 V because the withstand voltage of the MOSFET is 60 V. The load is 24 Ω resistors. The output voltage command is a full-wave rectified voltage with an amplitude of 30 V and 20 kHz which is used in WPT systems.

Figure 15 shows the waveforms of the gate-source voltage, the output voltage of the source follower, and the output voltage command of the test circuit. This result shows that the linear amplifier outputs the 20 kHz full-wave rectified voltage following the command value by feedback control. The output voltage is continuous without distortion or oscillation. From these results, it is confirmed that the controller and GDU for the proposed system enable the linear amplifier to stably output the high-frequency voltage used in the WPT system.
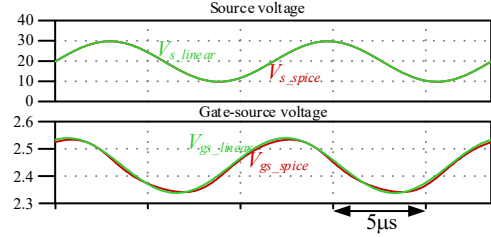

Fig. 10. Operation waveform of class-A source follower with small-signal equivalent model and MOSFET SPICE model.
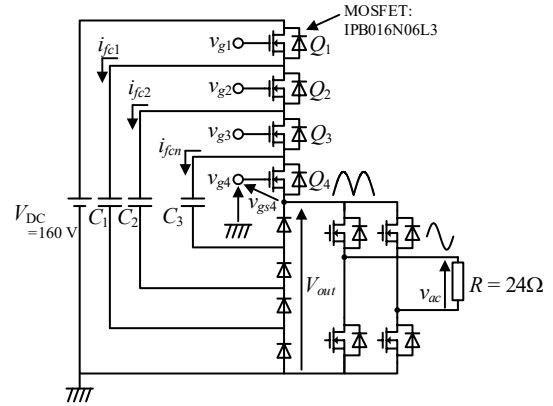

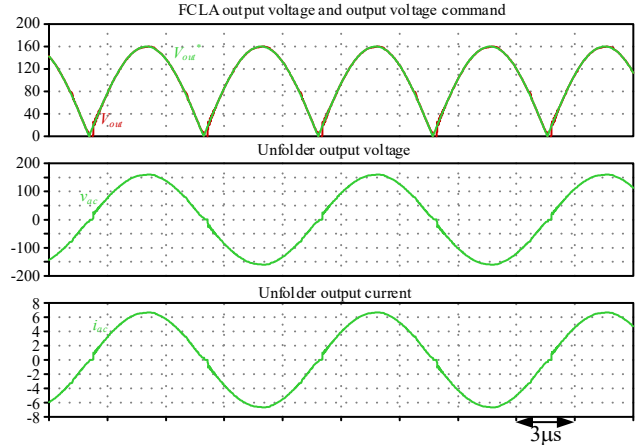Fig. 11. Simulation circuit of 4-sereies FCLA with unfolder.

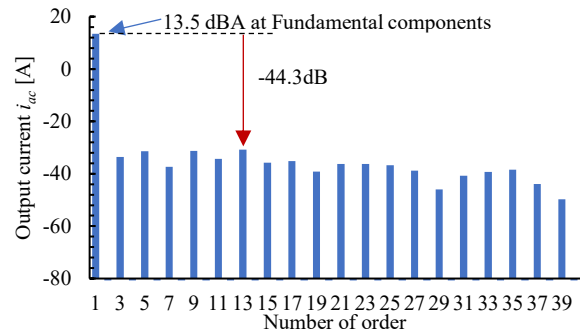Fig. 12. Operation waveform of FCLA with Unfolder.

Fig. 13. Harmonics analyze of output current.

VI. CONCLUSION

In this paper, the WPT system with a flying capacitor linear amplifier is proposed as a primary power supply to reduce the harmonics of radiated emissions. The FCLA applies a harmonic-free voltage to the transmission coils by using MOSFET in active-state. Because of this, the

proposed system significantly reduces the harmonics of the radiated emissions generated from the transmission coil. The configuration of the controller and GDU used in the proposed system is described and their stability analysis is presented. Furthermore, it is confirmed that the source follower is equivalent to single-series FCLA output the high-frequency voltage used for the WPT system.

In future work, the verification result of a WPT system with 16-series FCLA will be provided. The results of the harmonics analysis of the primary side current will be presented.
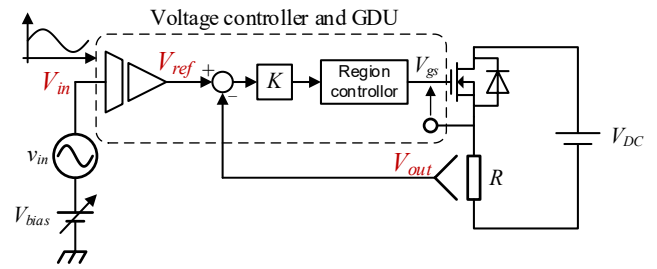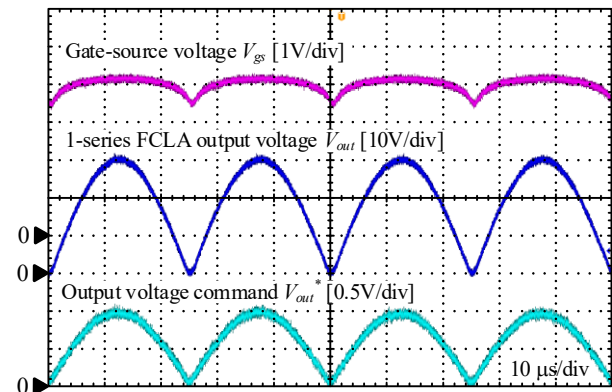

Fig. 14. Experimental circuit configuration.

Fig. 15. Operation waveform.

REFERENCES

[1] K. Nara, N. Madoiwa, K. Maeshiro, Y. Kaneko: "Wireless Power Transfer System with Ideal Transformer Characteristics Determined Solely by Coil Turns Ratio," IEEJ Journal of Industry Applications, Vol. 9, No. 6, pp. 656-662, (2020)

[2] H. Sumiya, E. Takahashi, N. Yamaguchi, K. Tani, S. Nagai, T. Fujita, H. Fujimoto: "Coil Scaling Law of Wireless Power Transfer Systems for Electromagnetic Field Leakage Evaluation for Electric Vehicles," IEEJ Journal of Industry Applications, Vol. 10, No. 5, pp. 589-597 (2021)

[3] H. Matsumoto, T. Zaitsu, R. Noborikawa, Y. Shibako, Y. Neba: "Control for Maximizing Efficiency of Three-Phase Wireless Power Transfer Systems At Misalignments," IEEJ Journal of Industry Applications, Vol. 9, No. 4, pp. 401-407 (2020)

[4] Ministry of Internal Affairs and Communications, Japan, "Inquiry of technical requirements for wireless power transfer system for EVs in technical requirements for wireless power transfer system in standards of International Special Committee on Radio Interference (CISPR)", (2015)

[5] N. Misawa : " Situation of EMC Limit Level of WPT for EV in CISPR", 2019 JSAE Annual Congress (Spring) Latest Trend of EV Charging System, No. 20194438, pp.15-20 (2019)

[6] S. Kim, G. A. Covic, J. T. Boys:"Comparison of Tripolar and Circular Pads for IPT Charging Systems," IEEE Transactions on Power Electronics, vol. 33, no. 7, pp. 6093-6103 (2018)

[7] M. Budhia, J. T. Boys, G. A. Covic, C. Huang: "Development of a Single-Sided Flux Magnetic Coupler for Electric Vehicle IPT Charging Systems," IEEE Tran. on Industrial Electronics, Vol. 60, No. 1, pp. 318-328, (2013)

[8] K. Furukawa, K. Kusaka, J. Itoh:"Low-EMF Wireless Power Transfer Systems of Four-Winding Coils with Injected Reactance-Compensation Current as Active Shielding," 2021 IEEE Applied Power Electronics Conference and Exposition (APEC), pp. 1618-1625 (2021)

[9] S. Cruciani, T. Campi, F. Maradei, M. Feliziani: "Active Shielding Design for Wireless Power Transfer Systems," in IEEE Transactions on Electromagnetic Compatibility, vol. 61, no. 6, pp. 1953-1960 (2019)

[10] H. Fujita, N. Yamashita, "Performance of a Diode-Clamped Linear Amplifier," IEEE Tran. on Power Electronics, Vol. 23, No. 2, pp. 824-831 (2008)

[11] Hidemine Obara, Tatsuki Ohno, Masaya Katayama, Atsuo Kawamura: "Flying-Capacitor Linear Amplifier with Capacitor Voltage Balancing for High-Efficiency and Low Distortion", IEEE Trans. on Industry Applications, Vol.57, No.1 (2021)